JOURNAL OF AEROSPACE COMPUTING, INFORMATION, AND COMMUNICATION
Vol. 1, July 2004

Simulation of Dynamic Contact Problems in Parachute Systems

Zhenlong Xu*, Michael Accorsi†, John Leonard†
University of Connecticut, Storrs, Connecticut 06269-2037

Contact phenomena are commonly observed in the operation of parachute systems. The effect of contact on parachute system performance is poorly understood and difficult to study experimentally. Computer simulations can provide an alternate method to evaluate these problems. In this paper, simulations of typical parachute contact phenomena are performed to evaluate the robustness of a previously developed structural model for modeling such problems. The structural model is based on a geometrically-nonlinear transient finite element formulation for membranes and cables that undergo large displacements and rotations and potentially "wrinkle" due to loss of tension. This model has been implemented in a parallel finite element code and is used with a computational fluid dynamics (CFD) code to perform fluid-structure interaction (FSI) simulations of parachute systems. In this paper, the inclusion of contact algorithms in this structural model is evaluated by performing simulations of parachute inflation, a parachute cluster, and an inflated parachute impacted by a foreign object. In these simulations, the structural model is used with prescribed pressures, which is considered to be a prerequisite to performing fully coupled FSI simulations of parachute systems with contact.

I. Introduction

PARACHUTE dynamics is a complex problem that involves large deformations and coupling between the parachute canopy and the surrounding airflow. Because of these complexities, this problem has traditionally been studied using a semi-empirical approach supplemented with laboratory and field-testing. However, this approach is both time-consuming and expensive. As computers become more powerful, large-scale numerical simulations become an attractive alternative for studying this problem.

Computer simulation of parachute dynamics can be performed using one of the following three models: a coupled fluid-structure interaction model (FSI), a stand-alone computational structural dynamics model (CSD) or a stand-alone computational fluid dynamics model (CFD). The most accurate approach is to conduct a fully coupled FSI simulation, however this is the most demanding from both a modeling and computational viewpoint. Useful results can be obtained through a CSD model with a prescribed fluid pressure field, or with a CFD model with a prescribed structural configuration. Examples of all these modeling approaches can be found in previous literature.

Fully coupled three-dimensional FSI simulations of parachute systems have recently been presented by Stein et al.,[1,2] Taylor,[3] and Strickland et al.[4] using a variety of different modeling approaches. Three-dimensional stand-alone CSD simulations with prescribed fluid pressure and drag have been presented, for example, by Zhou et al.[5] and Zhu et al.[6] for a variety of parachute systems and applications. Stand-alone CFD simulations that predict the flow field surrounding a canopy with prescribed geometry have recently been presented, for example, by Strickland et al.[7]

A very important issue in parachute systems is contact. Contact phenomena can occur at any time during a parachute operation, i.e., during deployment, inflation and terminal descent. Contact also occurs when several parachutes are used together in a cluster to support a single payload. In all these instances, the occurrence of contact

Presented as Paper 2003-2147 at the 17th AIAA Aerodynamic Decelerator Systems Technology Conference and Seminar, Monterey, California, 19-22 May 2003; received 21 January 2004; revision received 9 June 2004, accepted for publication 11 June 2004.
*Graduate Research Assistant, Department of Civil and Environmental Engineering.
†Professor, Department of Civil and Environmental Engineering.

may strongly affect the behavior of the parachute or the cluster, or result in complete failure of these systems. Despite its potential influence, contact phenomena in parachute systems has not been studied in any depth and remains very poorly understood.

Contact phenomena in large deformation problems such as parachute systems cannot be easily studied by experiments. Not only is it difficult to predict when and where contact occurs in such problems, it is also very difficult to analyze the evolution of contact through experiments. Contact between clustered parachutes during inflation was observed by Lee et al.[8] in laboratory tests, but no data to quantify the extent or duration of contact was measured. No additional laboratory or field data pertaining to parachute contact phenomena has been identified.

Computer simulations have the potential to provide valuable insights on parachute contact problems. Computer simulation of general contact problems have mostly concentrated on problems such as crashworthiness (for example, Elsner et al.[9]) and metal forming (for example, Nakamachi and Huo[10]), in which high impact speed and high structural stiffness are involved. In contrast, the study of contact problems involving highly flexible membrane structures has been limited primarily to airbag simulations (for example, Taylor[11] and Kang and Im[12]). To date, no major work involving simulation of contact in parachute systems has been performed.

In this paper, a contact simulation capability is incorporated into a CSD model that was previously developed to model parachute systems, and performance of this CSD-contact model is evaluated using simulations of typical parachute applications. The first application is the simulation of the inflation of a C-9 parachute starting from a highly folded initial configuration. In the second problem, contact within a cluster composed of three half-scale C-9 parachutes is modeled. The third simulation involves foreign object impact with an inflated T-10 parachute. The simulations utilize the CSD-contact model with prescribed pressures and drags to approximate the fluid forces, and serve primarily to evaluate the robustness of this model as opposed to making quantitative predictions. Future efforts will involve coupling the CSD-contact model with a CFD model to perform FSI simulations.

II. Methodology

The CSD model consists primarily of geometrically-nonlinear transient finite elements for highly flexible membranes and cables based on a total Lagrange formulation as described by Accorsi et al.[13] A variety of special features have been incorporated in this CSD model to tailor it for simulation of parachute systems. For example, a geometrically-nonlinear "wrinkling" algorithm was developed to model loss of tension in the membrane elements.[14] Additionally, special elements[5] needed to model specific features unique to parachute systems have been developed. FSI simulations of parachute systems that utilize this CSD model have been performed by a variety of investigators.[1,2]

The CSD model uses an implicit method (i.e., the HHT method[15]) to perform time integration. An implicit method was chosen instead of explicit methods for several reasons. First, it is well known that explicit methods are conditionally stable[16] and for typical parachute models the critical time step is found to be excruciatingly small. Although implicit methods require more calculations per time step than explicit methods (i.e., nonlinear iterations and factorization of the tangent stiffness matrix), the larger time step that can be used with implicit schemes offsets this disadvantage. Second, the nonlinear iteration required by implicit methods enforces satisfaction of equilibrium to a specified tolerance at each time step. This is particularly important for highly flexible and deformable structures, such as parachutes, to achieve accurate numerical solutions. For our numerical simulations, accuracy is measured by the ability to converge within a specified tolerance for each time step. Full Newton-Raphson iteration is used. We typically require the normalized iterative change in displacement vector magnitude to be less than 0.001 which is typically achieved in 3 to 10 iterations.

Contact mechanics algorithms were added to the CSD model using the geometrically-nonlinear contact formulation presented by Laursen and Simo[17] which provides expressions for the contact force vector and contact tangent stiffness matrix. Penalty and augmented Lagrange methods were both implemented and tested (see, for example, Laursen[18] for a discussion of these methods). For all our simulations, the penalty method provided stable and accurate results and was more computationally efficient than the augmented Lagrange approach. The favorable performance of the penalty method may be attributed to its use within the nonlinear iterative solver.

The CSD-contact model was implemented for a parallel computing environment. A detailed discussion of this implementation is given by Xu et al.[19] A simple decomposition is used where the element and system variables are distributed evenly among processors based solely on their numbering. Discussion of more sophisticated decompositions for parallel contact analysis is given by Brown et al.[20] and Plimpton et al.[21] The primary steps performed in the CSD-contact model are given in Table 1 along with the type of decomposition (i.e., the element equations and/or assembled system equations) needed to perform that step in parallel.

Table 1 Flowchart of CSD-contact model

Step	Computational Procedure	Type of Decomposition
(1)	Begin	
(2)	Begin Time Step	
(3)	Contact Search	Element Decomposition
(4)	Begin Newton-Raphson Iteration	
(5)	Calculate Local Element Equations (K, K_C, M, R, R_C)	Element Decomposition
(6)	Assemble System Equations	Element & System Decompositions
(7)	Solve System Equations	System Decomposition
(8)	Broadcast Updated System Information	System Decomposition
(9)	Check Newton-Raphson Convergence • if converged, go to (2) • if not converged, go to (4)	System Decomposition
(10)	End	

III. Numerical Simulations

Three applications are presented here to evaluate the robustness of the CSD-contact model for simulation of typical parachute systems. Prescribed pressure is used in all three problems to approximate the fluid forces. More realistic modeling of the fluid requires a FSI simulation; indeed, the next phase of our research effort will be to perform FSI simulations that include contact.

A. Inflation of a C-9 Parachute

Inflation is the phase when a parachute undergoes the largest amount of structural deformation. In contrast, even though a parachute may travel a very long distance during its terminal descent, its shape remains relatively unchanged during this period. Therefore, it is not surprising that a significant amount of contact occurs during the inflation phase. In a computer simulation, the inflation of a parachute cannot be realistically modeled without including contact.

In this simulation, inflation of a half-scale C-9 parachute is modeled. A flat "cut pattern" of the canopy mesh is show in Fig.1. The canopy has an outer radius of 7 ft. and an inner radius of 0.5 ft. The height of the parachute is 9.1 ft. The "folded" initial configuration is shown in Figs. 2 and 3. The finite element model for this problem contains 2046 nodes. It is composed of 3584 triangle membrane elements and 700 cable elements. The following figures (Figs. 4 – 8) show the inflation process of the parachute from a highly "folded" initial configuration to a fully deployed shape. Movie 1 is an animation extracted from the parachute inflation simulation.

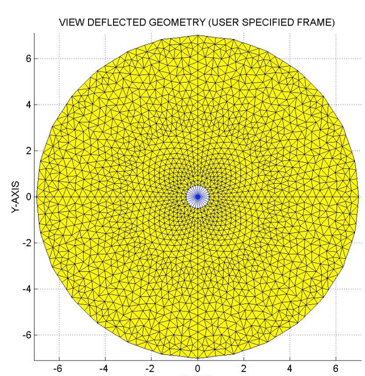

Fig. 1 Cut pattern of the C-9 parachute canopy.

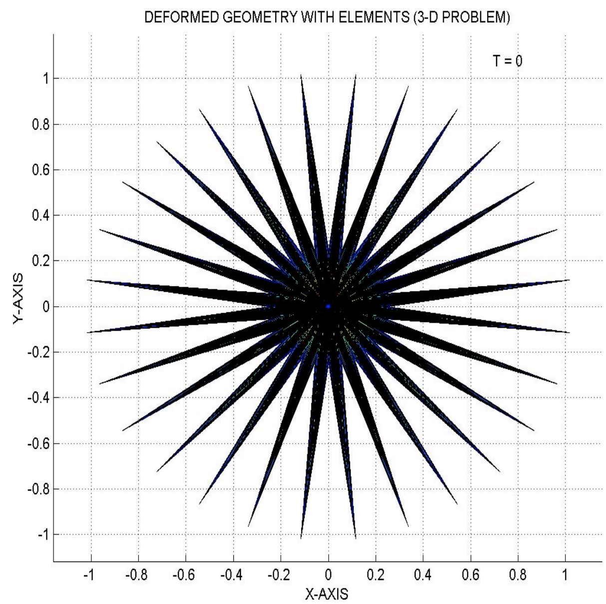

Fig. 2 Initial "folded" configuration of the C-9 parachute (top view).

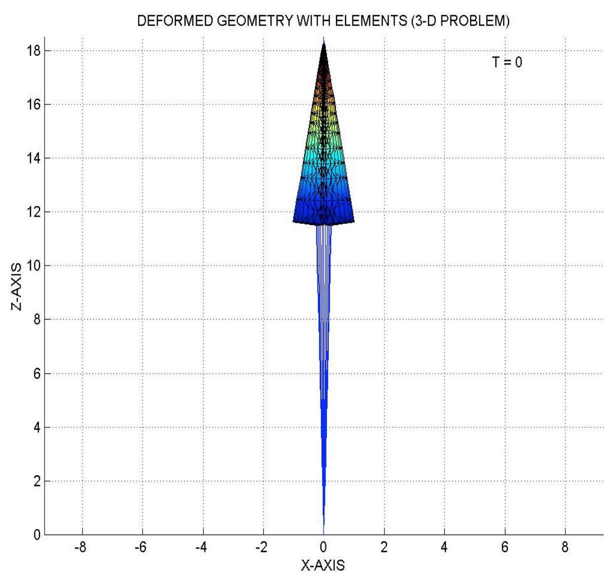

Fig. 3 Initial "folded" configuration of the C-9 parachute (side view).

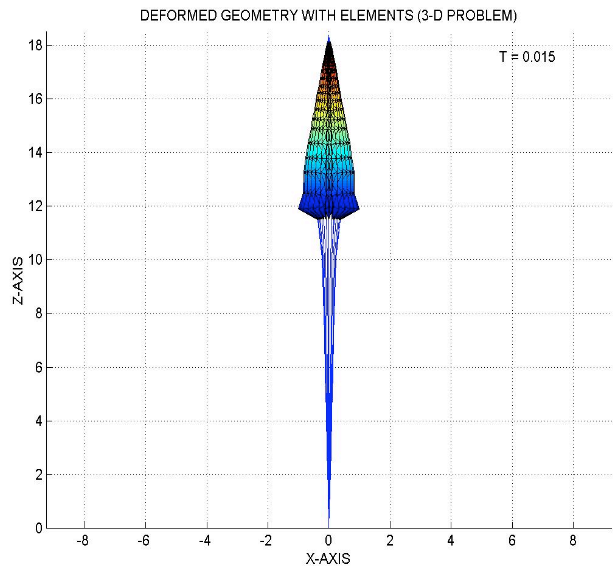

Fig. 4 Parachute configuration at t = 0.l015s.

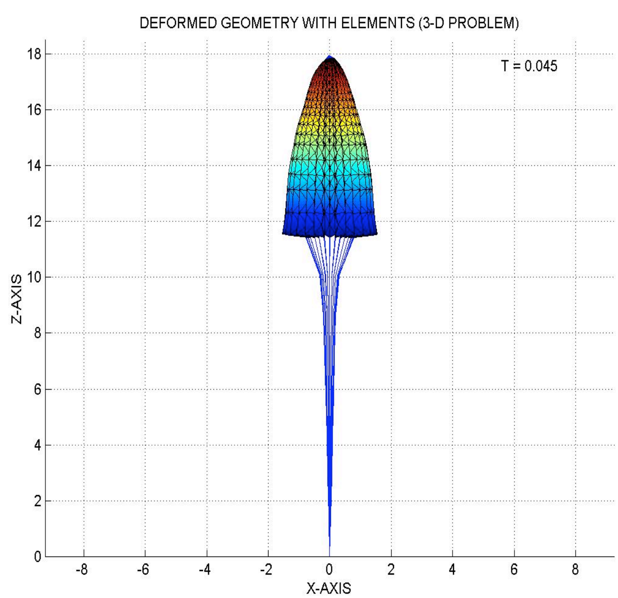

Fig. 5 Parachute configuration at t = 0.045s

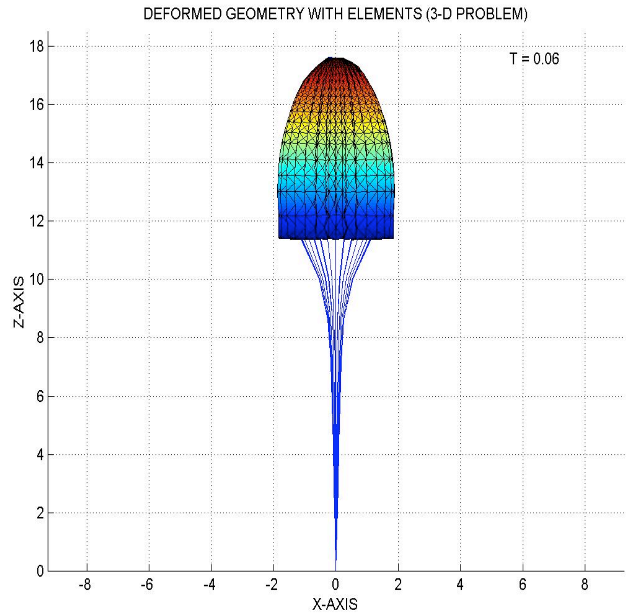

Fig. 6 Parachute configuration at t = 0.06 s.

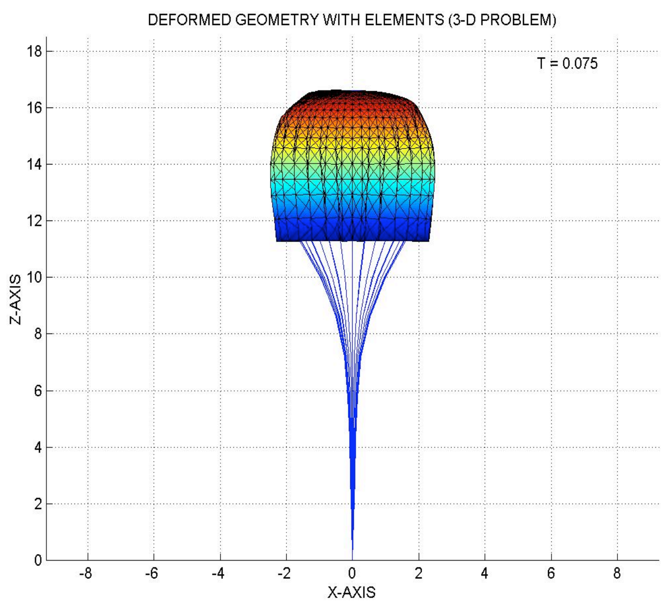

Fig. 7 Parachute configuration at t = 0.075s.

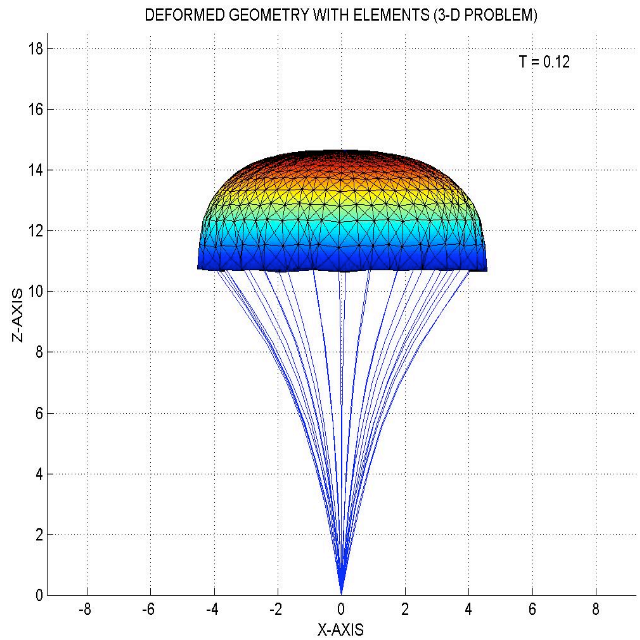

Fig. 8 Parachute configuration at t = 0.12 s.

To further illustrate the extent of contact in this problem, another inflation simulation was conducted using the same finite element model but without considering contact phenomena. The skirt configuration at several times during the inflation obtained from these two simulations is shown in the following figures for comparison.

Prior to contact, the two simulations give the same skirt shape as shown in Fig. 9. However, once contact occurs, the skirt shapes are drastically different with and without contact. While penetration between gores is obviously observed in Fig. 10, it is successfully prevented with the help of contact constraints in Fig. 11. As the inflation process proceeds, penetration becomes more severe in the simulation without contact. Each gore now spans into the space of several other gores, as shown in Fig. 12, while the shape is still well maintained with contact, as shown in Fig. 13.

Small penetration between neighboring gores is noticeable in Fig. 13. This is caused by the use of the penalty method for contact enforcement, in which small violation of contact constraints is practically allowed. It, however, should not be confused with the penetration observed in Fig. 12, which is the result of failing to consider contact entirely.

Figures 14 and 15 give two additional configurations of the skirt near the end of the contact process. Figures 16 and 17 are the skirt shapes after it comes out of the state of contact in both simulations. Although the two shapes are somehow similar at this stage, the path through which they have passed to reach here is dramatically different as previously seen. Movies 2 and 3 are animations of the skirts during inflation with and without contact, respectively.

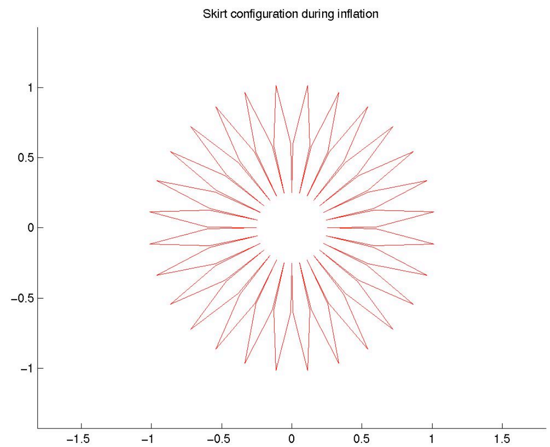

Fig. 9 Skirt configuration of the parachute at t = 0.0025 s (w/o contact).

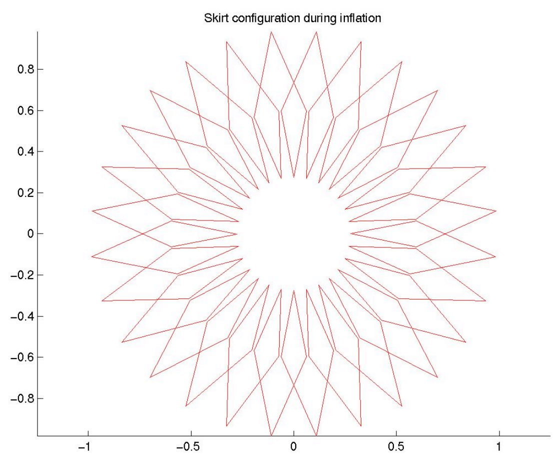

Fig. 10 Skirt configuration of the parachute at t = 0.005 s (w/o contact).

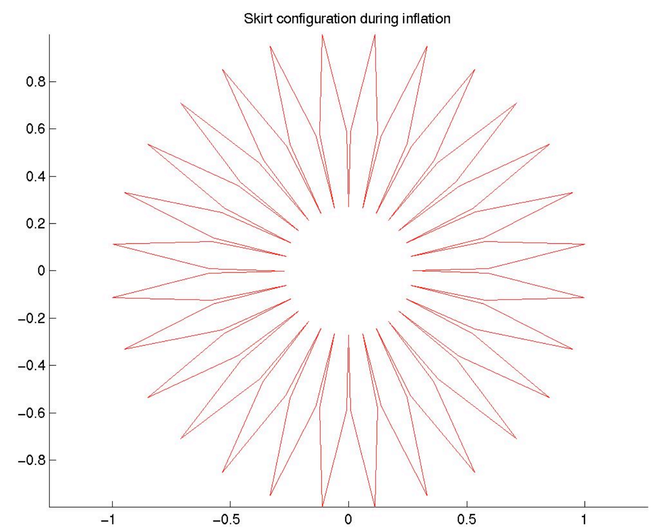

Fig. 11 Skirt configuration of the parachute at t = 0.005 s (w contact).

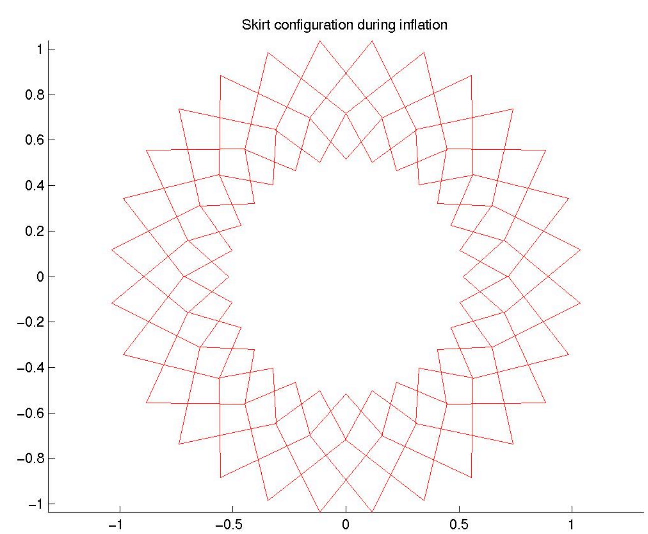

Fig. 12 Skirt configuration of the parachute at t = 0.025 s (w/o contact).

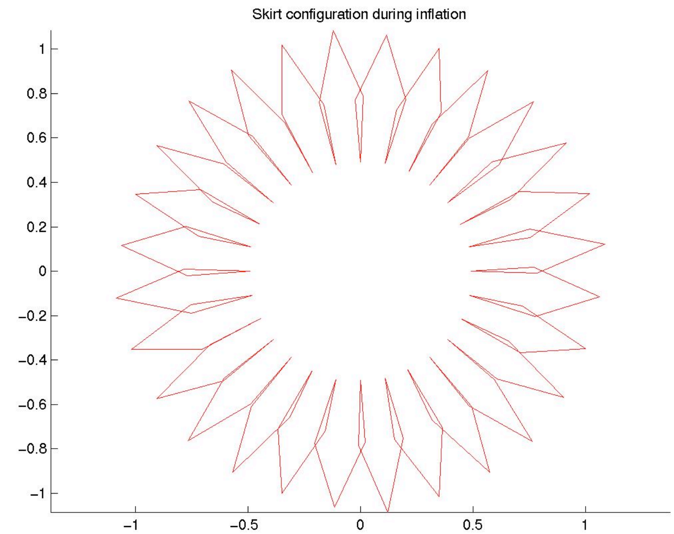

Fig. 13 Skirt configuration of the parachute at t = 0.025 s (w/ contact).

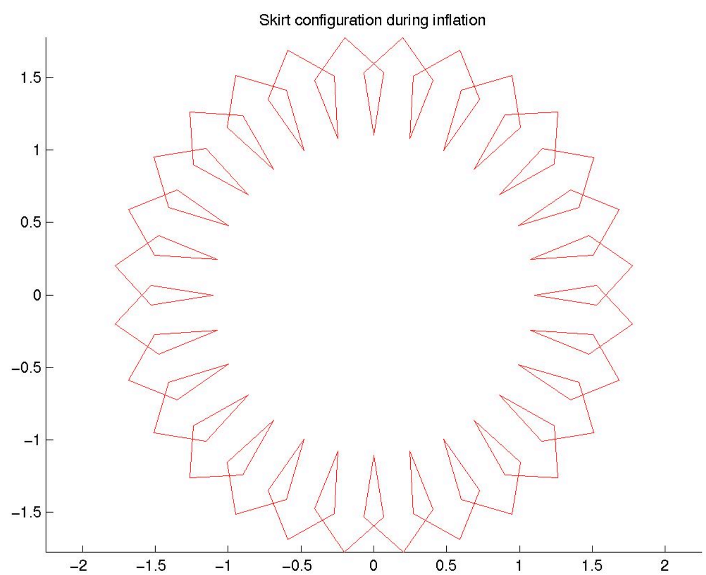

Fig. 14 Skirt configuration of the parachute at t = 0.07 s (w/o contact).

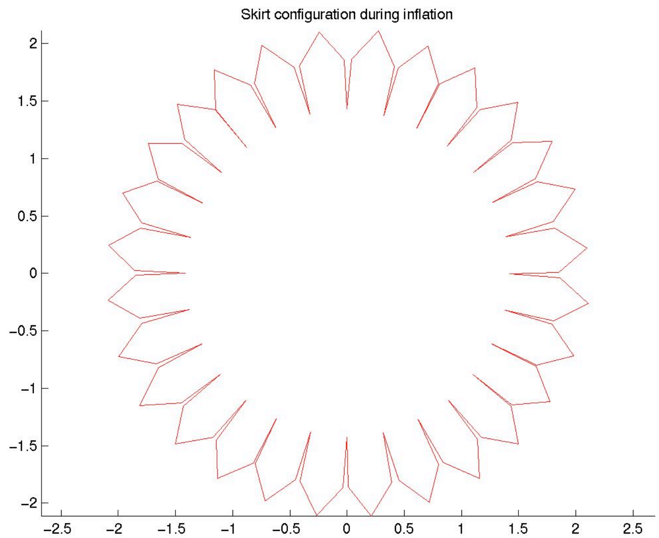

Fig. 15 Skirt configuration of the parachute at t = 0.07 s (w/o contact).

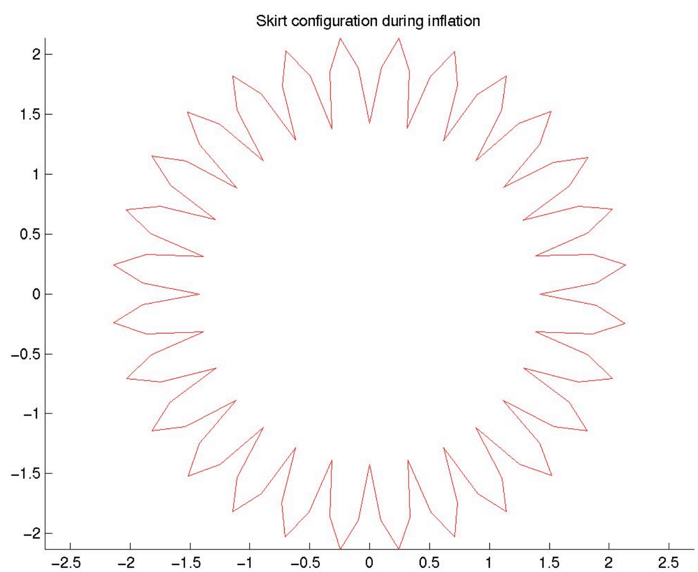

Fig. 16 Skirt configuration of the parachute at t = 0.0825 s (w/o contact).

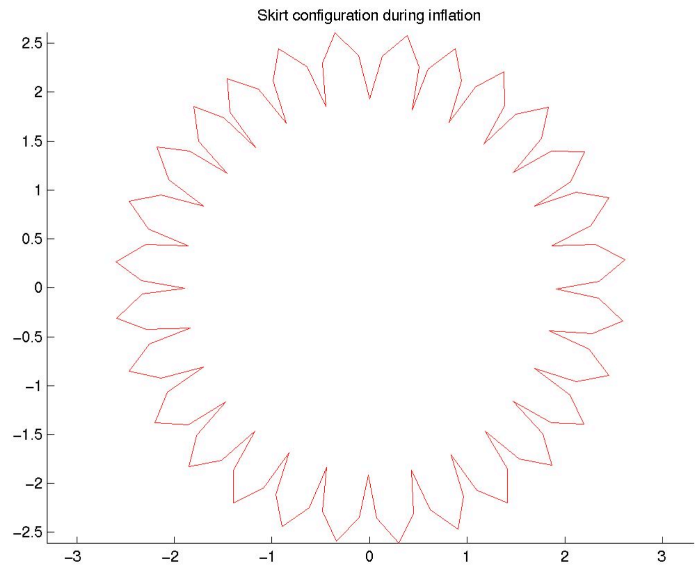

Fig. 17 Skirt configuration of the parachute at t = 0.0825 s (w/ contact).

B. Dropping of a Parachute Cluster Composed of Three C-9 Parachutes

Parachute clusters are generally used for dropping payloads of extremely high weight. Contact phenomena are commonly observed between different parachutes in a cluster. The occurrence of contact may adversely affect the stability of the cluster and therefore the success of the operation.

In this section, the process of dropping a cluster composed of three C-9 parachutes is studied. The finite element model for this problem consists of 6133 nodes, 11004 triangle membrane elements and 2352 cable elements.

Figures 18 and 19 are typical "snapshots" of the cluster during the computer simulation. Contact can obviously be observed over a very large extent of the canopies. In Fig. 19, "bulging" is observed at the top of the parachutes as a result of contact.

The evolution of contact in this cluster is further illustrated in Figs. 20 – 22. In these figures, the skirts of the three parachutes are plotted. Figure 20 depicts the cluster at an early stage when contact just starts to occur. In Fig. 21, contact has developed extensively in the cluster with the three parachutes contacting each other over a large percentage of the skirt. In Fig. 22, the extent of the contact has reduced as a result of the dynamic interaction between the three parachutes. Figure 23 shows the vertical descent of the cluster while maintaining contact between the parachutes. This is clearly a very dynamic process with the parachutes coming into contact then rebounding. At this point in the simulation, there is no damping on the model so this oscillatory behavior is not removed. Movies 4 and 5 are animations extracted from the simulations of cluster contact from the side view and top view, respectively.

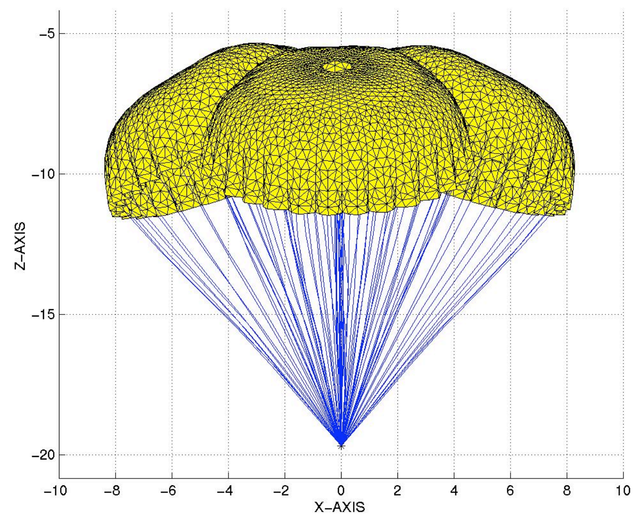

Fig. 18 Finite element model of the parachute cluster (side view).

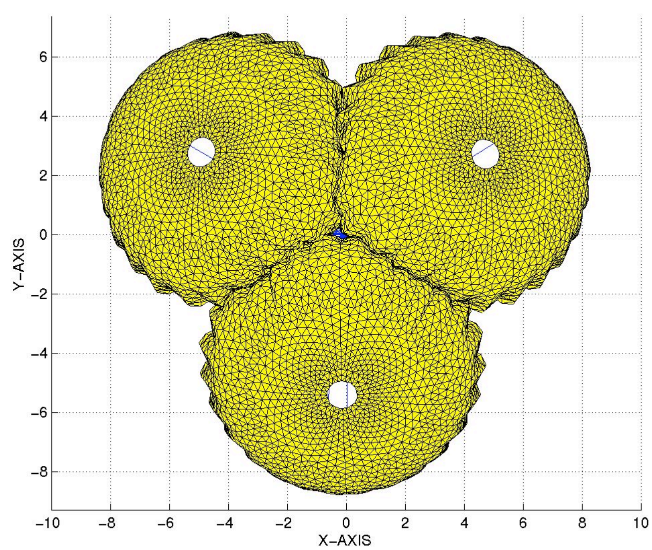

Fig. 19 Finite element model of the parachute cluster (top view).

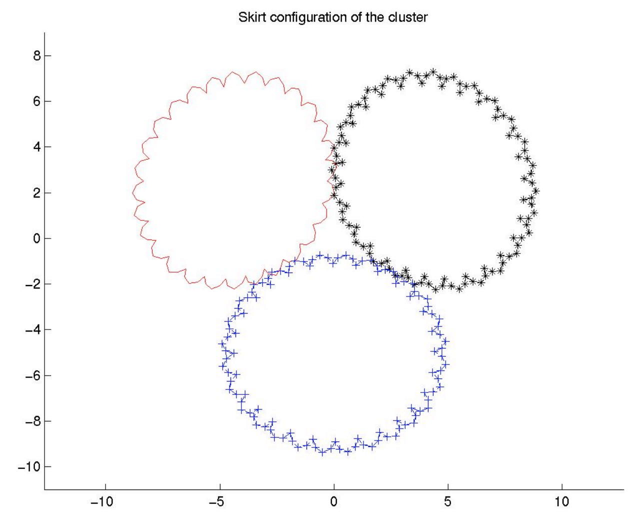

Fig. 20 Parachute skirt shapes in the cluster at t = 0.02 s.

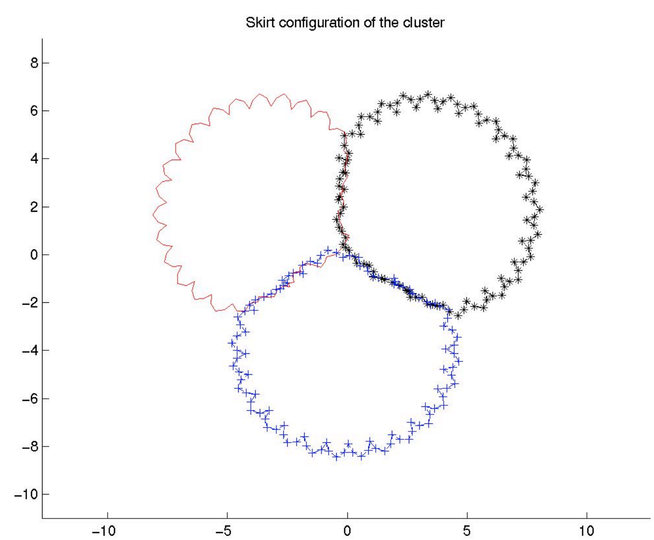

Fig. 21 Parachute skirt shapes in the cluster at t = 0.18 s.

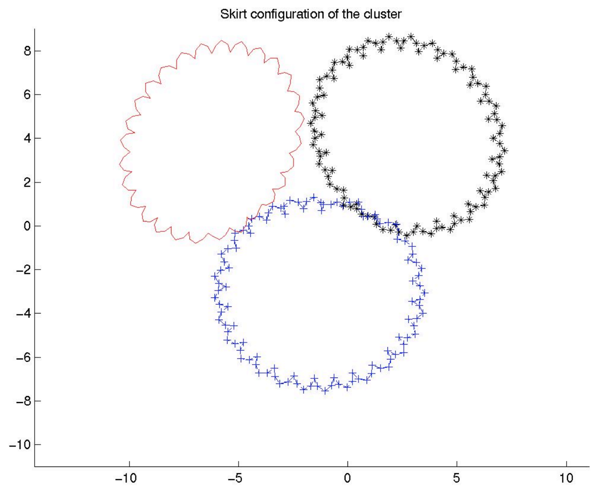

Fig. 22 Parachute skirt shapes in the cluster at t = 1.32 s.

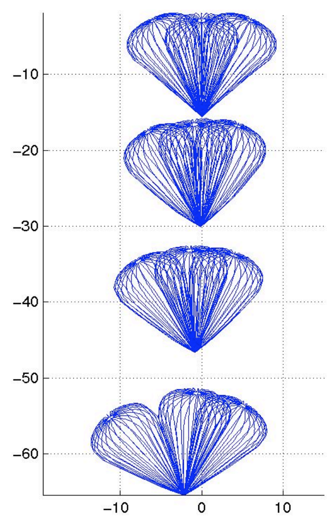

Fig. 23 Descent of the parachute cluster.

C. T-10 Personnel Parachute Under Foreign Object Impact

Although thought to be a rare incident, it is fairly common for parachutes to be impacted by foreign objects. Of most importance is when this happens with personnel parachutes, and human life is in immediate danger. During a massive deployment of troops, hundreds of paratroopers leave the aircraft in rapid succession and the likelihood of interference is quite high. Of particular interest is whether a contact event will cause collapse of an inflating canopy.

In this section, a T-10 personnel parachute under foreign object impact is simulated. To the best of our knowledge, this type of numerical simulation has not been previously performed. A fully inflated T-10 parachute is subjected to impact on the side by an object with a certain initial velocity. As shown in Fig. 24, the impacting body is suspended by cables to give it a pendulum type motion like that of a neighboring parachute. The parachute is modeled with 5970 triangle membrane elements and 1056 cable elements. The impacting object is modeled as a 3ft.×3ft. box. There are a total of 3190 nodes in this model.

The parachute is first inflated with a constant pressure. The object then impacts the parachute from the side with a velocity of 10ft/s. The behavior of the parachute is shown in Figs. 24 - 27. In Fig. 25, the parachute tips as it is impacted on the side. In Fig. 26, localized wrinkling is observed in the contact region. Figure 27 shows that the parachute is returning to a vertical position after the impact. It can be concluded that this impact is mild in nature, judging from the fact that the parachute maintains its inflated shape during and after the impact. In this simulation, however, the canopy pressure was assumed to be constant. The situation could be radically different if the fluid flow field was modeled more accurately, which again reinforces the need for FSI simulations. Movies 6 and 7 are animations extracted from the simulations showing the side view and top view, respectively, during and immediately after the impact.

In Fig. 28, the horizontal velocity history is plotted for three different positions of the parachute, i.e., the payload, a node in the impact region, and a node positioned across from the impact region. It can be seen that the change of velocity at the payload point is quite gradual and smooth due to its high inertia. In contrast, the velocities of the skirt nodes in the canopy change drastically in time. In particular, the nodal velocity in the contact region has a much larger range of fluctuation during the impact process than other parts of the canopy. While this phenomenon could be caused by the physical impact itself, it can also be attributed to the high flexibility of membrane elements in the numerical model. In a sense, this reflects the difficulty involved in simulating contact problems in compliant structures, in which numerical stability and convergence of nonlinear solutions are both difficult to achieve and maintain through time.

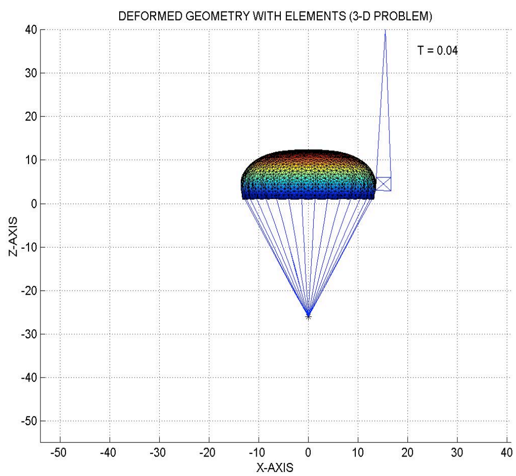

Fig. 24 T-10 parachute prior to impact.

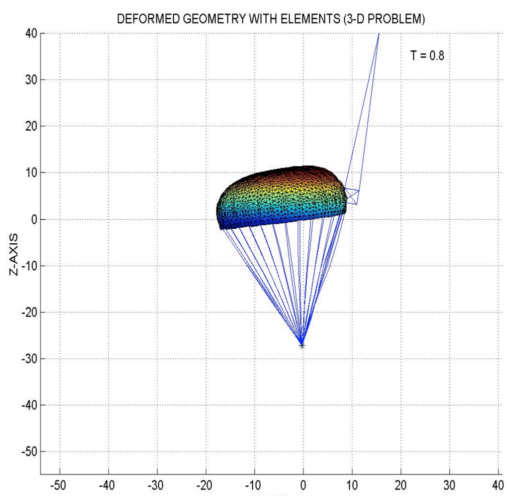

Fig. 25 T-10 parachute during impact (side view).

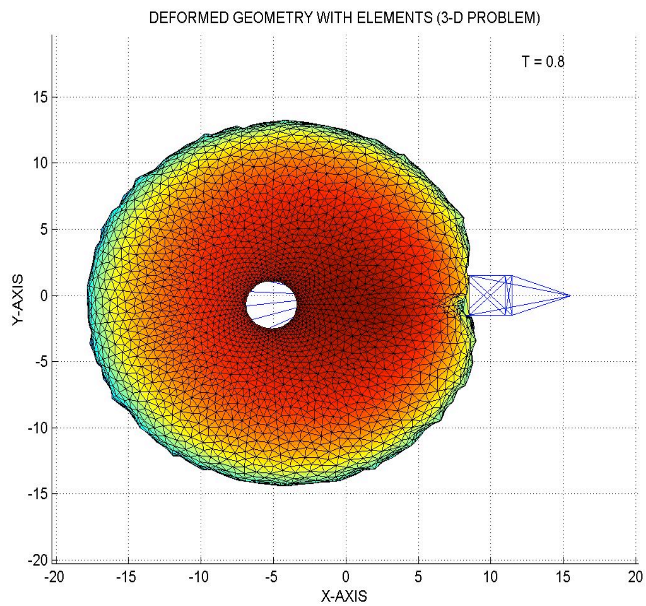

Fig. 26 T-10 parachute during impact (top view).

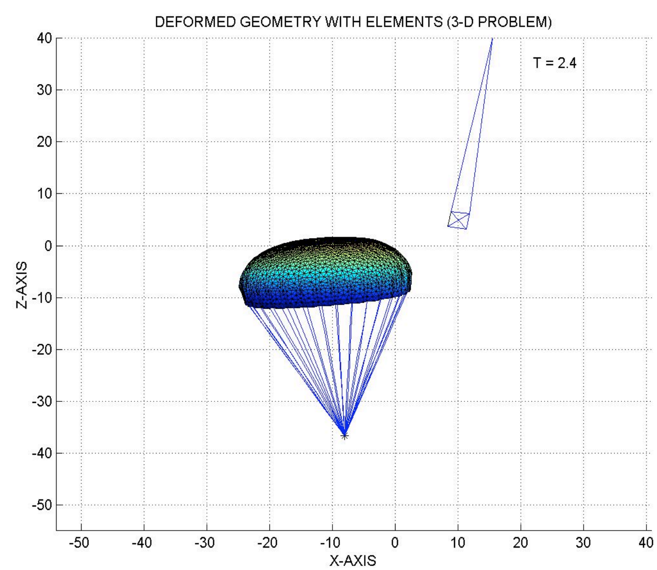

Fig. 27 T-10 parachute after impact.

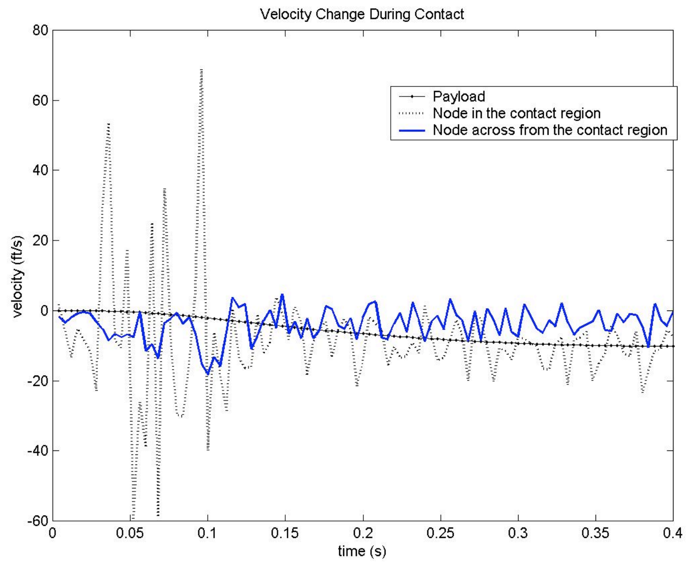

Fig. 28 Velocity at different positions of the parachute.

IV. Parallel Computational Performance

Evaluation of the parallel efficiency for the CSD-contact model was performed for the C-9 inflation problem presented in the preceding section. This problem was selected because it involves a large number of contacts during the simulation. This simulation was performed on an SGI Origin 2000 platform without partitioning the finite element mesh. The simulations were performed twice, with and without the contact algorithms, with the number of processors ranging from 1 to 50. The speedup versus number of processors is shown in Fig. 29 where each case is normalized by the CPU time for a single processor (1293 seconds for no contact and 11,137 seconds with contact). For a single processor, the simulation with contact requires 8.6 times more CPU time than the simulation without contact, which is indicative of the computationally intensive nature of contact problems.

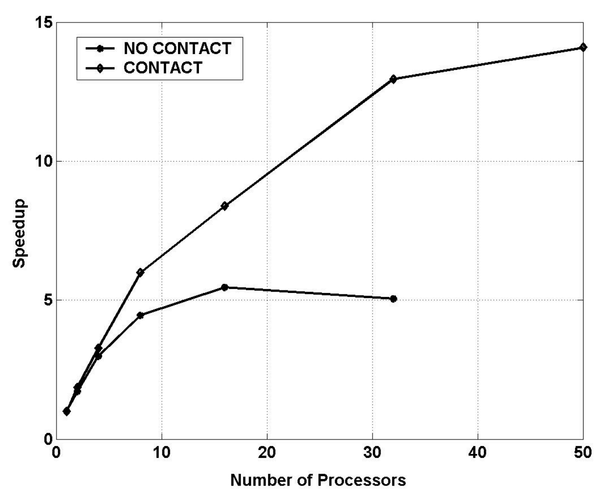

Fig. 29 Speedup vs number of processors with and without contact.

The leveling off of both curves occurs when the computational costs associated with communication between the processors outweighs the benefits of using additional processors. For this relatively small example problem, this effect occurs with 16 processors for the simulation without contact. For the simulation with contact, speedup increases continuously up to 50 processors.

V. Conclusions

In this paper, a computational structural dynamics (CSD) model that includes contact mechanics was evaluated for simulation of parachute problems that involve contact. The robustness of this model was tested by performing three large-scale simulations that represent typical parachute applications. In general, the CSD-contact model performed very well. The simulations were stable for long time durations and the good convergence characteristics indicate that good numerical accuracy is achieved.

The simulations were performed with prescribed pressures to approximate the fluid forces. Although the results from these simulations are physically realistic, true modeling of the fluid field using computational fluid dynamics (CFD) is needed before the model can be used for quantitative predictions. The preliminary CSD simulations performed here, however, strongly suggest that the CSD is robust enough to be used in a fully coupled FSI model. Future efforts will focus on coupling the CSD-contact model with a CFD code to perform FSI simulations of parachute systems with contact events.

Acknowledgment

This paper is based upon work supported by, or in part by, the U.S. Army Research Office under grant number DAAD19-99-1-0235. The authors also acknowledge support under a DoD HPC Challenge Project.

References

[1]Stein, K., Benney, R., Tezduyar, T., Sathe, S., Charles, R., and Kumar, V., "Simulation of Parachute Dynamics During Control Line Input Operations," AIAA Paper 2003-2151, *17th AIAA Aerodynamic Decelerator Systems Technology Conference*, 19-22 May 2003, pp. 358-363.

[2]Stein, K., Benney, R., Kumar, V., Tezduyar, T., Thornburg, E., Kyle, C., and Nonoshita, T., "Aerodynamic Interaction Between Multiple Parachute Canopies," AIAA Paper 2001-2004, *A Collection of the 16th AIAA Aerodynamic Decelerator Systems Conference Technical Papers*, 21-24 May 2001, pp. 77-84.

[3]Taylor, T., "An Investigation of the Apparent Mass of Parachutes Under Post Inflation Dynamic Loading Through the use of Fluid Structure Interaction Simulations," AIAA Paper 2003-2104, *17th AIAA Aerodynamic Decelerator Systems Technology Conference*, 19-22 May 2003, pp. 31-39.

[4]Strickland, J., Porter, V., and Homicz, G., "Fluid- Structure Coupling for Lightweight Flexible Bodies," AIAA Paper 2003-2157, *17th AIAA Aerodynamic Decelerator Systems Technology Conference*, 19-22 May 2003, pp. 404-411.

[5]Zhou, B., Accorsi, M., Benney, R., and Charles, R., "Two Specialized Structural Elements for Airdrop System Modeling," *17th AIAA Aerodynamic Decelerator Systems Technology Conference*, 19-22 May 2003, pp. 364-371.

[6]Zhu, Y., Moreau, M., Accorsi, M., Leonard , J., and Smith, J., "Computer Simulation of Parafoil Dynamics," AIAA Paper 2001-2005, *A Collection of the 16th AIAA Aerodynamic Decelerator Systems Conference Technical Papers*, 21-24 May 2001.

[7]Strickland, J., Gossler, A., Homicz, G., Porter, V., and Wolfe, W., "On the Development of a Gridless Inflation Code for Parachute Simulations," AIAA Paper 2001-2000, *A Collection of the 16th AIAA Aerodynamic Decelerator Systems Conference Technical Papers*, 21-24 May 2001, pp. 42-51.

[8]Lee, C., Lanza, J., and Buckley, J., "Experimental Investigation of Clustered Parachutes Inflation," AIAA Paper 1997-1478, *14th AIAA Aerodynamic Decelerator Systems Technology Conference*, 3-5 June 1997, pp. 187-202

[9]Elsner, B., Galbas, G., Gorg, B., Kolp, O., and Lonsdale, G., "A Parallel Multi-Level Approach for Contact Problems in Crashworthiness Simulation," *Parallel Computing: State-of-the-Art and Perspectives*, Elsevier Science, 1996.

[10]Nakamachi, E., and Huo, T., "Dynamic-Explicit Elastic Plastic Finite-Element Simulation of Hemispherical Punch-Drawing of Sheet Metal," *Engineering Computations*, Vol. 13, 1996, pp. 327-338

[11]Taylor, T., "Explicit Finite Element Analysis of Fabric Systems, a Comparison to Test Data" AIAA Paper 2001-2003, *A Collection of the 16th AIAA Aerodynamic Decelerator Systems Conference Technical Papers*, 21-24 May 2001, pp. 69-76.

[12]Kang, S., and Im, S., "Finite Element Analysis of Dynamic Response of Wrinkling Membranes," *Computer Methods in Applied Mechanics and Engineering*, Vol. 173, 1999, pp. 227-240

[13]Accorsi, M., Leonard, J., Benney, R., and Stein, K., "Structural Modeling of Parachute Dynamics," *AIAA Journal*, Vol. 37, 1999, pp. 139-146

[14]Lu, K., Accorsi, M., and Leonard, J., "Finite Element Analysis of Membrane Wrinkling," *International Journal for Numerical Methods in Engineering,* Vol. 50, 2001, pp. 1017-1038.

[15]Hughes, J. R. T., *The Finite Element Method: Linear Static and Dynamic Finite Element Analysis*, Prentice-Hall, Englewood Cliffs, NJ, 1987.

[16]Bathe, K.-J., *Finite Element Procedures*, Prentice-Hall Inc., Englewood Cliffs, NJ, (1996)

[17]Laursen, T., and Simo, J., "Continuum-Based Finite Element Formulation for the Implicit Solution of Multi-body, Large Deformation Frictional Contact Problems," *International Journal for Numerical Methods in Engineering*, Vol. 36, 1993, pp. 3451-3485

[18]Laursen, T., *Computational Contact and Impact Mechanics*, Springer-Verlag, Berlin, 2002.

[19]Xu, Z., Accorsi, M., and Leonard, J., "Parallel Contact Algorithms For Nonlinear Implicit Transient Analysis," *Computational Mechanics* (in press).

[20]Brown, K., Attaway, S. Plimpton, S., and Hendrickson, B., "Parallel Strategies for Crash and Impact Simulations," *Computer Methods in Applied Mechanics and Engineering*, Vol. 184, 2000, pp. 375-390.

[21]Plimpton, S., Attaway, S., Hendrickson, B., Swegle, J., Vaughan, C., and Gardner, D., "Parallel Transient Dynamics Simulations: Algorithms for Contact Detection and Smoothed Particle Hydrodynamics," *Journal of Parallel and Distributed Computing*, Vol. 50, 1998, pp. 104-122.